Author: Goeij, Bart E.C.G. de
Title: Antibody-drug conjugates in cancer
Issue Date: 2016-04-13

3 High turnover of Tissue Factor enables efficient intracellular delivery of antibody-drug conjugates

► Mol Cancer Ther. 2015 May;14(5):1130-40.

► Bart ECG de Goeij[1], David Satijn[1], Claudia M Freitag[1], Richard Wubbolts[2], Wim K Bleeker[1], Alisher Khasanov[3], Tong Zhu[3], Gary Chen[3], David Miao[3], Patrick HC van Berkel[1] and Paul WHI Parren[1,4,5]

1 Genmab, Yalelaan 60, 3584 CM, Utrecht, The Netherlands

2 Department of Biochemistry and Cell Biology, Faculty of Veterinary Medicine, Utrecht University, Yalelaan 2, 3584 CM, Utrecht, The Netherlands

3 Concortis Biosystems Corp., San Diego, 11760 Sorrento Valley, CA 92121, USA

4 Dept. of Cancer and Inflammation Research, Institute of Molecular Medicine, University of Southern Denmark, Odense, Denmark

5 Dept. of immunohematology and Blood Transfusion, Leiden University Medical Center, 2333 ZA Leiden, The Netherlands

ABSTRACT

Antibody drug conjugates (ADC) are emerging as powerful cancer treatments that combine antibody-mediated tumor targeting with the potent cytotoxic activity of toxins. We recently reported the development of a novel ADC that delivers the cytotoxic payload monomethyl auristatin E (MMAE) to tumor cells expressing tissue factor (TF). By carefully selecting a TF-specific antibody that interferes with TF:FVIIa-dependent intracellular signaling, but not with the pro-coagulant activity of TF, an ADC was developed (TF-011-MMAE/HuMax-TF-ADC) that efficiently kills tumor cells, with an acceptable toxicology profile.

To gain more insight in the efficacy of TF-directed ADC treatment we compared the internalization characteristics and intracellular routing of TF with the epidermal growth factor receptor (EGFR) and human epidermal growth factor receptor 2 (HER2). Both in absence and presence of antibody, TF demonstrated more efficient internalization, lysosomal targeting and degradation than EGFR and HER2. By conjugating TF, EGFR and HER2 specific antibodies with duostatin-3, a toxin that induces potent cytotoxicity upon antibody-mediated internalization but lacks the ability to induce bystander killing, we were able to compare cytotoxicity of ADCs with different tumor specificities. TF-ADC demonstrated effective killing against tumor cell lines with variable levels of target expression. In xenograft models, TF-ADC was relatively potent in reducing tumor growth compared to EGFR- and HER2- ADCs. We hypothesize that the constant turnover of TF on tumor cells, makes this protein especially suitable for an ADC approach.

INTRODUCTION

Therapeutic antibodies are currently used in the clinic to treat a variety of diseases, including cancer. The tumor-killing capacity of therapeutic antibodies can be greatly enhanced by conjugation with cytostatic toxins, this way combining antibody-mediated tumor targeting with the potent cytotoxic activity of toxins. This was also demonstrated through the FDA approval of brentuximab vedotin, a CD30 specific antibody coupled to the potent microtubule disrupting agent monomethyl auristatin E (MMAE), for the treatment of patients with Hodgkin's lymphoma or anaplastic T-cell lymphoma [1]. In addition, the approval of trastuzumab emtansine (T-DM1), an ADC composed of the HER2 antibody trastuzumab and the tubulin inhibitor maytansine (DM1), for the treatment of patients with HER2-positive breast cancer [2,3] emphasizes that the potential of ADCs is not limited to hematological malignanices. The number of ADCs in clinical development has markedly increased in the last couple of years. This includes the development of HuMax-TF-ADC (TF-011-MMAE), a novel

ADC designed to deliver the cytotoxic payload MMAE to tumor cells expressing tissue factor (TF) [4].

Tissue factor, also called thromboplastin, factor III or CD142, is aberrantly expressed in many types of cancers including NSCLC [5], colorectal cancer [6], genito-urethal [7,8] and gyneacological cancers [9-11], pancreatic cancer [12], head and neck cancer [13], glioma [14] and metastatic breast cancer [15]. Under physiological conditions, TF is expressed by fibroblasts, pericytes and smooth muscle cells in the sub-endothelial vessel wall. In these cells, the majority of TF is localized in intracellular pools and remains sequestered from circulating factor VII (FVII) until vascular integrity is disrupted or until TF expression is induced [16-18]. Upon vascular damage, TF binds activated FVII (FVIIa) and forms the proteolytically active TF:FVIIa complex that can initiate the coagulation pathway. The TF:FVIIa complex can also activate cells by cleavage of the G-protein coupled receptor protease-activated receptor 2 (PAR2) thereby inducing an intracellular signaling cascade that promotes proliferation, thrombosis and angiogenesis [19]. This makes TF an interesting yet challenging target for cancer immunotherapy.

TF-011-MMAE was designed to specifically target tumor cells that aberrantly express TF, without interfering with the role of TF in coagulation. TF-011-MMAE showed potent anti-tumor activity in xenograft models derived from a broad range of solid cancers, and an acceptable safety profile in non-clinical toxicology studies [4]. TF-011-MMAE and unconjugated TF-011 induced efficient antibody-dependent cell-mediated cytoxicity and inhibition of TF:FVIIa-dependent intracellular signaling, both of which may contribute to the anti-tumor activity of TF-011-MMAE. However, MMAE-mediated tumor cell killing was shown to be the dominant mechanism of action *in vivo*. This indicates that TF is a highly suitable target for the intracellular delivery of cytoxic agents through an ADC. To gain more insight in the target characteristics, particularly the internalization characteristics of TF and TF-specific antibodies, that contribute to the efficacy of TF-directed ADC treatment, we compared TF-specific ADCs with ADCs directed against HER2 and EGFR. HER2 is a well-known and clinically validated ADC target [3,20], and an EGFR antibody conjugated with DM1 through a non-cleavable linker system is currently being evaluated in a phase I clinical study. Antibodies targeting TF, HER2 and EGFR were conjugated with the cytotoxic compound duostatin-3, which blocks tubulin polymerization. This toxin lacks the ability to induce bystander killing and therefore only affects target-positive cells. Because tumor antigens are often heterogeneously expressed and therefore not always accessible to ADC treatment, an ADC capable of inducing bystander killing may be preferred from an efficacy point-of-view [4]. However, to study the target requirements needed for optimal intracellular delivery of cytotoxic agents, we selected a drug-linker combination that only affects antigen expressing cells.

By comparing *in vitro* and *in vivo* cytotoxicity of ADCs targeting TF, HER2 and EGFR we found that TF-ADC was more effective compared to ADCs targeting the EGF-receptor family. TF-ADC induced relatively potent tumor cell killing, even in cell lines where TF expression was lower than expression of HER2 or EGFR. Confocal microscopy analysis demonstrated faster and enhanced transport of TF-antibodies into lysosomes of tumor cells compared to EGFR and HER2 antibodies. Strikingly, also without antibody treatment, large quantities of TF were found to internalize and colocalize with markers of endosomes and lysosomes, indicating that TF was constitutively being replenished. Therefore, it seems that the high turnover of TF on tumor cells, inherent to its biological role, makes this protein specifically suitable for an ADC approach.

MATERIALS AND METHOD

Cell lines

Human SK-OV-3 (ovarian cancer), AU565 (breast adenocarcinoma) and HCC1954 (breast ductal carcinoma) cells were obtained from American Type Culture Collection (ATCC). Human A431 (epithelial squamous carcinoma) and Jurkat (T-cell leukemia) cells were obtained from the Deutsche Sammlung von Mikroorganismen und Zellkulturen (DSMZ). SK-OV-3 cells were cultured in Minimal Essential Medium Eagles (ATCC) containing 10% heat inactivated calf serum (Hyclone). HCC1954, A431 and Jurkat cells were cultured in RPMI 1640 (Lonza) containing 10% heat inactivated calf serum. AU565 cells were cultured in RPMI 1640 supplemented with 10% heat inactivated calf serum, 1% sodium bicarbonate (Lonza), 0.5% natrium pyruvate (Lonza) and 0.5% glucose (Sigma). To guarantee cell line authenticity, cell lines were aliquoted and banked, and cultures were grown and used for a limited number of passages before starting a new culture from stock. Cell lines were routinely tested for mycoplasma contamination. TF, HER2 and EGFR cell surface expression was quantified by QIFIKIT analysis (DAKO) according to the manufacturer's guidelines, using a mouse anti-human TF antibody (CLB), mouse anti-human HER2 antibody (R&D) and mouse anti-human EGFR antibody (BD) as described in supplementary method S1.

Antibody generation and conjugation

Human IgG1κ monoclonal antibodies were generated in human antibody transgenic mice; HuMAb® mice (Medarex), using hybridoma technolgy [21]. Tissue Factor antibodies were previously described [4]. In brief, TF-011 binds TF, interferes with FVIIa binding and inhibits ERK-phosphorylation. TF-111 binds TF and partially interferes with FVIIa binding and ERK-phosphorylation. The HER2 mAbs 153 and 005 were described by de Goeij et al. [22]. Both antibodies bound to epitopes distinct from those recognized by trastuzumab and pertuzumab. Upon binding to HER2, mAb 153 inhibits ligand-induced HER2 proliferation. mAb 005 has no effect on HER2 induced

proliferation. The EGFR mAbs zalutumumab and nimotuzumab (Biacon) both inhibit ligand binding and EGFR driven proliferation. Zalutumumab does so with high affinity [23], while nimotuzumab blocks EGF binding with low affinity [24].

Duostatin-3 conjugated antibodies were generated by covalent conjugation of valine-citrulline-duostatin-3 on antibody lysine groups as described in WO/2013/173391. The synthesis of duostatin-3 is also described in the supplementary method S2. Each resulting duostatin-3 conjugated ADC contained an average of 2 drug molecules per antibody, as determined by hydrophobic interaction chromatography (HIC). Duostatin-3 conjugated antibodies were referred to as TF-ADC, HER2-ADC and EGFR-ADC. TF-011 was also conjugated with maleimidocaproyl-valine-citrulline-*p*-aminobenzoyl-monomethyl auristatin E (vcMMAE, licensed from Seattle Genetics) on cysteine groups in the antibody hinge region, to generate TF-011-MMAE (HuMax-TF-ADC), as described [4]. This ADC was referred to as TF-011-MMAE throughout the manuscript. TF-011-MMAE contained an average of 4 drug molecules per antibody.

Confocal microscopy

Cells were grown on glass coverslips (Thermo Fisher Scientific) at 37°C for 16 hours. In case of antibody stimulation, cells were pre-incubated 1 hour with 50 µg/mL leupeptin (Sigma) to block lysosomal activity followed by 1 or 16 hours incubation with 1 µg/mL EGFR-, HER2- or TF-antibody. Cells were fixed, permeabilizedand incubated 45 min with mouse anti-human TF (CLB), HER2 (R&D) and EGFR (BD Pharmingen) antibodies, followed by goat anti-mouse IgG1-FITC (DAKO) to identify receptors, or goat anti-human IgG1-FITC (Jackson) to stain for human EGFR-, HER2- and TF- antibodies. Endosomes were stained with rabbit anti-human transferrin (Life Technology) and goat anti-rabbit IgG-Alexa-568 (Bio-connect), lysosomes were stained with mouse anti-human CD107a-APC (BD). Finally, coverslips were mounted (Calbiochem) on microscope slides and imaged with a Leica SPE-II confocal microscope (Leica Microsystems) equipped with LAS-AF software. 12-bit grayscale TIFF images were analyzed for colocalisation using MetaMorph® software (Molecular Devices). Colocalisation was calculated as the FITC pixel intensity overlapping with APC (lysosomes) or AlexaFluor568 (endosomes) and expressed as percentage of total FITC intensity.

Surface protein downmodulation assay

SK-OV-3 and A431 cells were seeded in 96-wells non-binding plates (Greiner), 100,000 cells/well, in serum-free culture medium, with or without 100 µM monensin (Dako) to block recycling of endosomes (30 minutes, 37°C) [25]. Next, human TF-, HER2- and EGFR- antibodies (10 µg/mL), EGF (Biosource, 50 ng/mL) or FVIIa (Novoseven, 100 ng/mL) were added for 3 hours (37°C). Remaining TF, HER2 or EGFR at the plasma membrane were stained with non-competing mouse TF (CLB), HER2 (R&D) and EGFR antibodies (BD) (30 min, 4°C), followed by incubation with goat anti-mouse IgG-FITC (Jackson, 30 min, 4°C). Mean Fluorescence Intensity (MFI) of

FITC was measured on a flow cytometer (BD). Quantification of cell surface proteins was done using QIFIKIT® (Dako) according to the manufacturer's instructions [26].

Total protein downmodulation assay

Cells were seeded (100,000 cells/well) in 96-wells culture plates (Greiner). After 4 hours cells were pre-incubated with 100 μM chloroquine (Sigma) or 100 μg/mL leupeptin (Sigma, 30 min, 37°C), followed by incubation with 10 μg/mL human TF, HER2 or EGFR antibodies. After 48 hours, cells were washed, lysed and total protein levels were quantified using bicinchoninic acid (BCA) protein assay reagent (Pierce), according to manufacturer's instruction. Next, ELISA plates (Greiner) were coated with 1 μg/mL mouse anti-human EGFR (Millipore), rabbit anti-human HER2 (Cell Signalling Technology) or mouse anti-human TF (CLB), blocked with 2% chicken serum (Hyclone) and incubated with 50 μL cell lysate. Subsequently, EGFR, HER2 and TF were detected with mouse anti-human EGFR-biotin (Leica Technologies, 0.5 μg/mL), goat anti-human HER2-biotin (R&D, 50 ng/mL) and goat anti-human TF-biotin (R&D, 0.5 μg/mL). The reaction was visualized as described [27].

Intracellular antibody accumulation

Cells were incubated with 5 μg/mL FITC-conjugated antibodies at either 4°C or 37°C. At the indicated time points, cells were transferred on ice to stop internalization and washed with ice-cold phosphate buffered saline (B.Braun Melsungen). 50 μL ice-cold acid wash buffer (0.2M glycine [Sigma], 4M urea [Sigma], pH2.0) was added for 5 minutes to remove extracellular bound antibodies and removed through centrifugation. Remaining FITC-fluorescence, originating from internalized FITC-conjugated antibodies, was measured using flow cytometry.

CypHer5E internalization assay

Cells were seeded in 96-well plates (Greiner, 20,000 cells/well) and cultured overnight at 37°C. Ice-cold culture medium with or without 100 μM chloroquine (Sigma) was added for 1 hour at 4°C, to trap internalized antibody in endosomal compartments. Next, 1 μg/mL HER2, EGFR or TF antibody, conjugated with CypHer5E according to manufacturer's instructions (GE Healthcare), was added. CypHer5E is a pH-sensitive dye which is non-fluorescent at basic pH (extracellular: culture medium) and fluorescent at acidic pH (intracellular: endosomes, lysosomes). After 30 minutes, the cells were washed and fresh culture medium (37°C) was added. The cells were incubated 24 hours at 37°C. At indicated time points MFI of internalized CypHer5E was measured per well using homogeneous Fluorometric Microvolume Assay Technology (FMAT, Applied Biosystems). As read out, fluorescence per cell was multiplied with the number of positive cells per well (counts x fluorescence).

Cytotoxicity assay

Mixed cell cultures were treated with ADC to simultaneously determine the amount of target cell kill and bystander kill. HER2, EGFR and TF expressing tumor cells were used as target cells and seeded (5,000 cells/well) in 96-well culture plates. Antigen negative Jurkat cells were used as bystander cells and added to the plate (20,000 cells/well). To discriminate between both cell populations, Jurkat cells were labelled with CellTraceTM carboxyfluorescein diacetate succinimidyl ester (CFSE) according to manufacturer's instructions (Invitrogen). Next, serially diluted ADCs (10-0.000001 µg/mL) were added and the cells were incubated 4 days at 37^{0}C. Cells were harvested and viability was assessed through live/dead staining on a flow cytometer. Target cell kill was plotted as the percentage of viable CFSE-negative cells. Bystander kill was plotted as the percentage of viable CFSE-positive cells.

Alternatively, 500,000 CFSE labeled cells were cultured in T25 flasks (Greiner) in presence of 2 µg/mL ADC. After 3 days the viable cells were harvested and analyzed for antigen expression using mouse TF (CLB), HER2 (R&D) and EGFR antibodies (BD) and goat anti-mouse IgG1-APC (Jackson). Each sample was spiked with 10,000 CFSE-negative Jurkat cells. During flow cytometry analysis, the CFSE-negative Jurkat cells were gated and 3,000 events were measured in this gate, while all events were stored and analyzed.

Tumor xenograft models

6-11 week old female SCID mice (C.B-17/IcrPrkdc-scid/CRL) were purchased from Charles River. Subcutaneous tumors were induced by inoculation of 5 x 10^6 cells in the right flank of the mice. Tumor volumes were calculated from digital caliper measurements as 0.52 x length x width^2 (mm^3). When tumors reached 200-400 mm^3, mice were grouped into groups of 7 mice with equal tumor size distribution and mAbs were injected intraperitoneally at indicated time points (1 or 4 mg/kg). During the study, blood samples were collected into heparin-containing tubes to confirm the presence of human IgG in plasma. IgG levels were quantified using a Nephelometer (Siemens Healthcare). Mice that did not show human IgG in plasma were excluded from the analysis. Some mice developing ulcerations not related to tumor size, were euthanized for ethical reasons before the end of the study, which is indicated by the censored data points.

Statistical analysis

Data analysis was done using GraphPad Prism 5 software. Group data were reported as mean ± SD. One-way ANOVA was applied for statistical analysis. Statistical analysis of xenograft studies was done with one-way ANOVA at the last day that all groups were complete. Mantel-Cox analysis of Kaplan-Meier curves was performed to analyze statistical differences in progression-free survival time.

RESULTS

Tissue Factor distribution in unstimulated tumor cells

In healthy tissue, TF is primarily expressed in intracellular pools and remains sequestered from circulating FVII [17,18,28]. To determine TF distribution in cancer cells we applied confocal microscopy. For this, we selected two cell lines based on aberrant expression of HER2 and TF (SK-OV-3, ovarian cancer) or EGFR and TF (A431, epithelial carcinoma), as depicted in Table 1. The cells were grown on glass coverslips, left unstimulated and stained for TF, EGFR and HER2. Markers of recycling endosomes (i.e. transferrin) and lysosomes (i.e. LAMP1) were included to determine compartmentalization of the different proteins. Figure 1A-C demonstrates that, in resting SK-OV-3 cells, TF is primarily localized intracellularly and partially colocalizes with the lysosomal marker LAMP1. EGFR and HER2 staining on the other hand was mainly localized to the plasma membrane.

Cell line	Origin	TF (molecules/cell)	EGFR (molecules/cell)	HER2 (molecules/cell)
HCC1954	Breast cancer	400,000	100,000	600,000
A431	Epithelial cancer	200,000	500,000	30,000
SK-OV-3	Ovarian cancer	100,000	50,000	200,000
AU565	Breast cancer	20,000	100,000	500,000

TABLE 1 *Number of molecules on plasma membrane*. Average number of EGFR, HER2 and TF molecules expressed on the cell surface, calculated with quantitative flow cytometry as described in supplementary method S1.

Also in A431 cells (Figure 1D) and HCC1954 cells (Supplementary Figure S1), TF was more abundantly present in lysosomes as compared to EGFR and HER2, suggesting that TF has a high turnover in these tumor cells. This was confirmed by ELISA where total protein levels of TF, EGFR and HER2 were measured in absence and presence of inhibitors of lysosomal degradation (Figure 1E). Total protein levels of EGFR and HER2 were unaffected by addition of chloroquine, an inhibitor of endosomal acidification [29] or leupeptin, an inhibitor of lysosomal proteases. However, TF protein levels were increased over 2-fold when lysosomal degradation was blocked with chloroquine, indicating that TF is continuously transported from endosomal to lysosomal compartments to undergo degradation.

The enhanced colocalisation of TF with transferrin (Figure 1D) suggests that at least a part of the intracellular TF pool originated from the plasma membrane [30]. Therefore we next investigated downmodulation of surface expressed receptors using quantitative flow cytometry. SK-OV-3 cells were incubated with the TF ligand FVIIa or the EGFR ligand EGF, after which residual receptor expression was quantified.

Monensin was added to block transport of intracellular receptors to the cell surface and thereby trap internalized proteins in the cell. Figure 1F shows that FVIIa alone had no effect on surface expression of TF, whereas monensin significantly reduced TF expression, indicating that TF is constitutively recruited from intracellular pools to the plasma membrane. Previous reports have described the internalization of TF in presence of FVIIa [16,31], our data demonstrate that TF is also internalized in absence of FVIIa. EGF on the other hand induced significant downmodulation of surface expressed EGFR which was in line with previous reports [32], while HER2 expression was unaffected by EGF and monensin.

In summary, unlike EGFR and HER2, TF was continuously internalized and degraded, even in resting tumor cells. This suggests that the efficacy of TF-specific ADCs may be at least partly related to the endogenous internalization characteristics of TF.

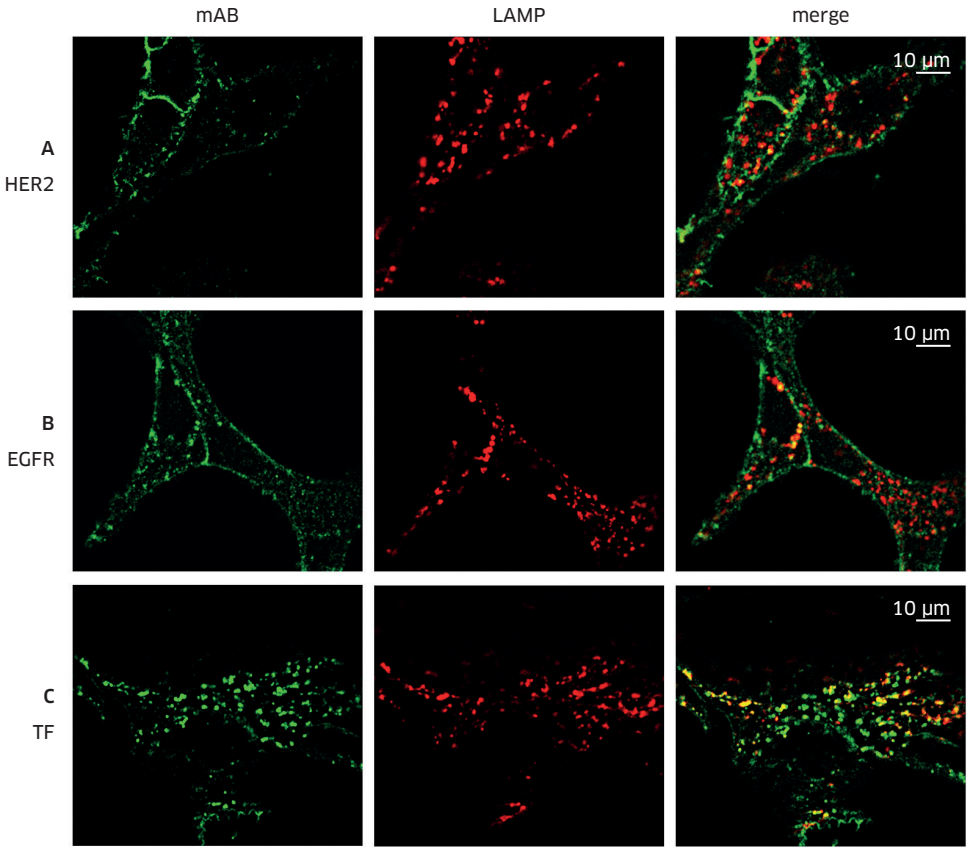

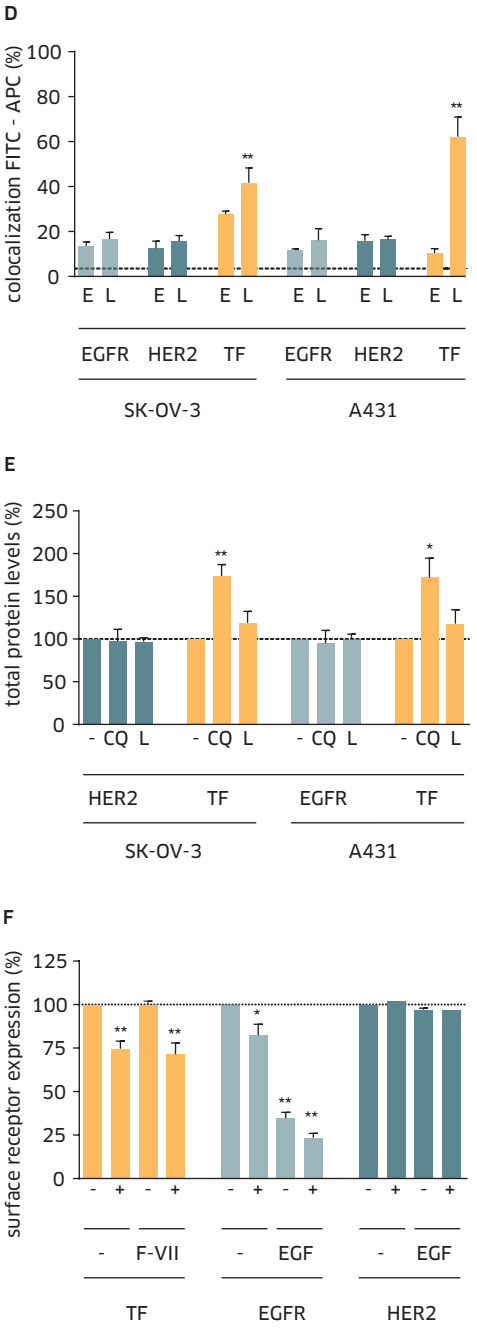

FIGURE 1 *Distribution of HER2, EGFR and TF in unstimulated tumor cells.* **(A-C, page 44)** Confocal microscopy images (8-bit) of unstimulated SK-OV-3 cells. The left panel shows staining of HER2 **(A)**, EGFR **(B)** and TF **(C)** with murine antibodies and goat anti-mouse IgG-FITC (green). In the middle panel lysosomes were stained with mouse anti-human LAMP1-APC (red). The right panel shows the overlay (yellow). **(D)** Quantification of endosomal and lysosomal receptor colocalisation. Each bar represents 4 different 12-bit images ± standard deviation. E=endosomes L=lysosomes. **(E)** Downmodulation of total protein expression. Cells were incubated for 2 days with 100 µM chloroquine or 100 µg/mL leupeptin, after which protein levels were measured with ELISA and expressed as percentage compared to untreated cells. Data shown are mean ± standard deviatin. **(F)** Surface protein downmodulation on SK-OV-3 cells measured with quantitative flow cytometry. Cells were preincubated 30 minutes with (+) or without (-) monensin and incubated an additional 3 hours with 50 ng/mL EGF or 100 ng/mL FVIIa. Surface expression of remaining TF, EGFR and HER2 was quantified and plotted as percentage relative to untreated cells. Data shown are mean ± standard deviation. *P<0.05, **P<0.001

Antibody binding to TF triggers internalization of mAb/TF-complexes

For certain receptors, antibody binding results in internalization of the Ab/receptor-complex [32]. To investigate whether Ab/TF-complexes were internalized, we incubated SK-OV-3 and A431 cells for three hours at 37°C with antibodies directed against TF, EGFR and HER2. The cells were cooled to 4°C and remaining extracellular proteins were quantified using non-competing murine TF, EGFR and HER2 antibodies. Figure 2A demonstrates that TF-011 and TF-111 induced significant downmodulation of extracellular TF, which was not observed with Fab fragments of mAb TF-011 or the TF physiological ligand FVIIa. The tested EGFR and HER2 antibodies had no effect on extracellular expression of EGFR and HER2 respectively. The experiment was also performed in presence of the recycling inhibitor monensin. For EGFR and TF, this further decreased extracellular expression (data not shown).

Next, it was investigated whether antibody-mediated downmodulation of total protein levels. SK-OV-3 and A431 cells were incubated for 2 days with EGFR, HER2 and TF antibodies, lysed and subjected to ELISA to measure the degree of protein. Figure 2B shows that TF-011 induced downmodulation of total TF protein in both cell lines. Also a slight reduction of EGFR protein levels was observed upon incubation with EGFR antibody zalutumumab, but no effect on HER2 protein levels was observed with any of the HER2 antibodies.

To exclude that the reduced protein levels depicted in Figure 2A result from antibody-induced shedding of TF, intracellular accumulation of FITC-conjugated antibodies was assessed to confirm that Ab/TF-complexes were indeed internalized. Cells were incubated with FITC-conjugated antibodies at 37°C for 0-9 hours. Prior to flow cytometry analysis, extracellular FITC-conjugated antibodies were removed through acid wash and residual FITC fluorescence, originating from internalized FITC-conjugated antibodies, was measured on a flow cytometer. As depicted in figure 2C and D, both TF antibodies showed accumulation of FITC fluorescence over time, demonstrating that these antibodies were efficiently internalized.

TF/TF-011 complexes are rapidly targeted to the lysosomes

For an ADC-approach, it is typically required that internalized antibodies traffic to lysosomes where cellular proteases can initiate drug release [33]. Using confocal microscopy, lysosomal transport of TF, EGFR and HER2 antibodies was analyzed. SK-OV-3 and A431 cells were incubated with the indicated antibodies, and after 1 or 16 hours cells were fixed, permeabilized and stained with FITC-conjugated goat-α-human IgG1. After one hour, TF-011 already demonstrated clear internalization and lysosomal colocalisation (Figure 3A). EGFR antibody zalutumumab was also internalized after one hour, but the internalized antibody had not yet reached the lysosomes (Figure 3C), while HER2 antibody 005 only stained at the plasma membrane (Figure 3E). After 16 hours, all antibodies demonstrated substantial internalization and ly-

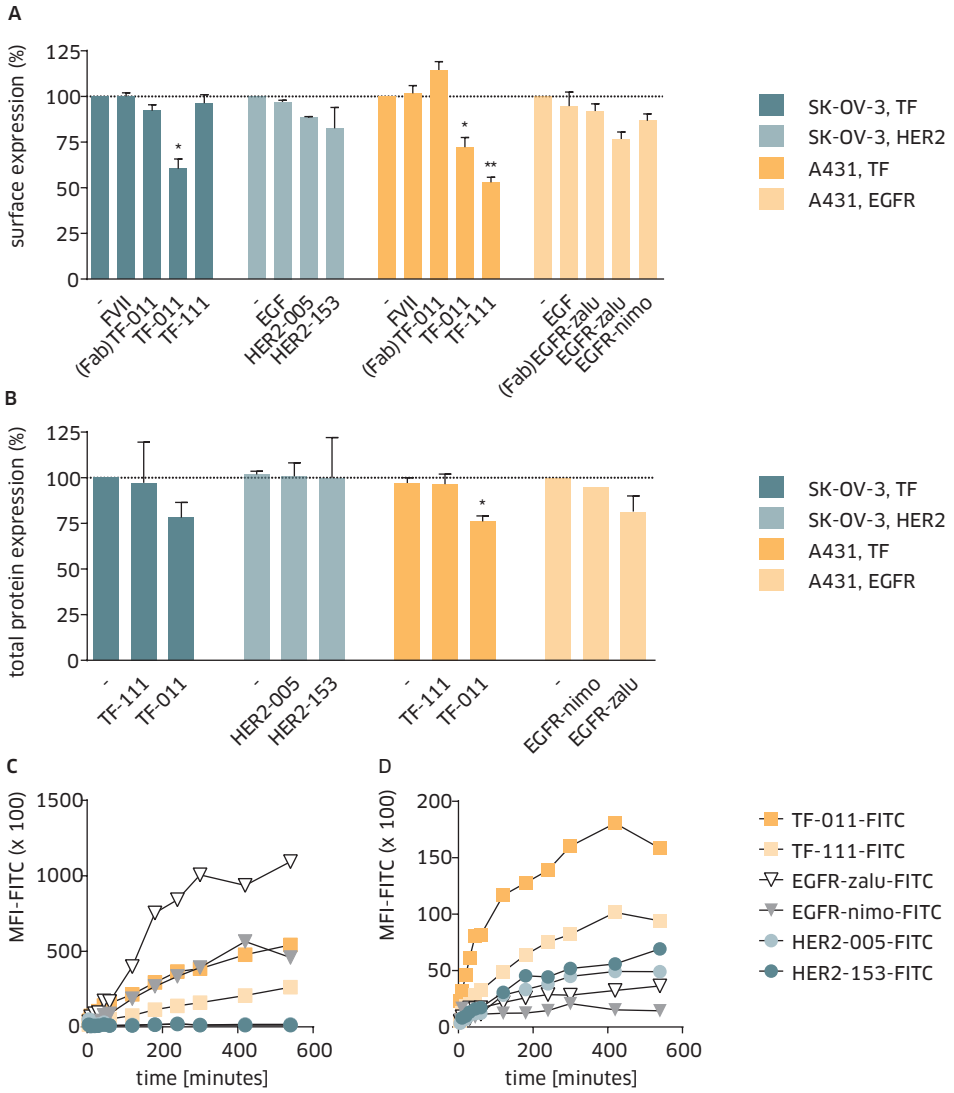

FIGURE 2 Antibody-mediated internalization and downmodulation of TF, EGFR and HER2. **(A)** Downmodulation of surface expressed proteins measured with flow cytometry. SK-OV-3 and A431 cells were incubated with 10 µg/mL antibody. After 3 hours, remaining surface expression of the different receptors was analyzed with quantitative flow cytometry and expressed as percentage relative to untreated cells. **(B)** Downmodulation of total protein levels. SK-OV-3 and A431 cells were incubated with 10 µg/mL antibody. After two days protein levels were measured with ELISA and expressed as percentage compared to untreated cells. Data shown are mean ± standard deviation. **(C-D)** Intracellular accumulation of FITC-conjugated antibodies measured with flow cytometry. **(C)** A431 and **(D)** SK-OV-3 cells were incubated with 10 µg/mL Ab-FITC at 4°C and 37°C. At the indicated timepoints, extracellular bound Ab-FITC was removed through acid wash and MFI of intracellular FITC was analyzed with flow cytometry. One representative experiment out of three is shown. *P<0.05, **P<0.001.

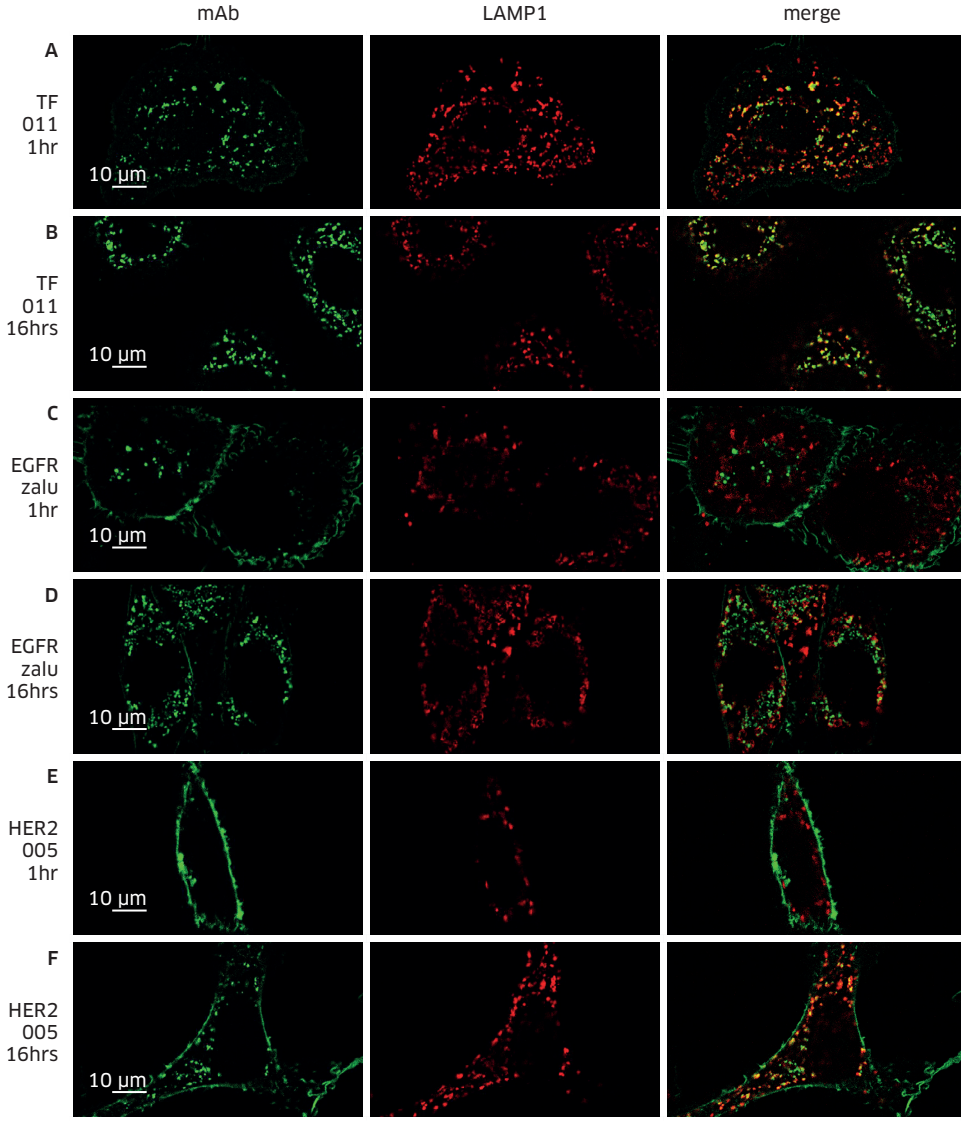

FIGURE 3 *Lysosomal colocalisation of TF, EGFR and HER2 antibodies*. **(A-F)** Confocal microscopy analysis of SK-OV-3 **(A-B, E-F)** and A431 **(C-D)** cells demonstrating fast and increased lysosomal transport of TF-011. Lysosomes were stained with mouse anti-human LAMP1-APC (red). Zalutumumab (anti-EGFR), 005 (anti-HER2) and TF-011 (anti-TF) were detected with goat anti-human IgG1-FITC (green). **(G)** Arbitrary units [AU] represent the total pixel intensity of antibody overlapping with the lysosomal marker LAMP1, divided by the total pixel intensity of LAMP1. Data shown are mean ± standard deviation of 4 images. **(H-K)** Lysosomal targeting of CypHer5E conjugated mAbs. SK-OV-3 cells, preincubated with or without 100 µM chloroquine, were incubated with CypHer5E-conjugated antibodies: TF-011 **(H)**, zalutumumab **(I)**, 005 **(J)** and 153 **(K)**. At the indicated time points, CypHer5E fluorescence was measured using homogeneous Fluorometric Microvolume Assay Technology. The grey area indicates antibody present in lysosomal compartments.

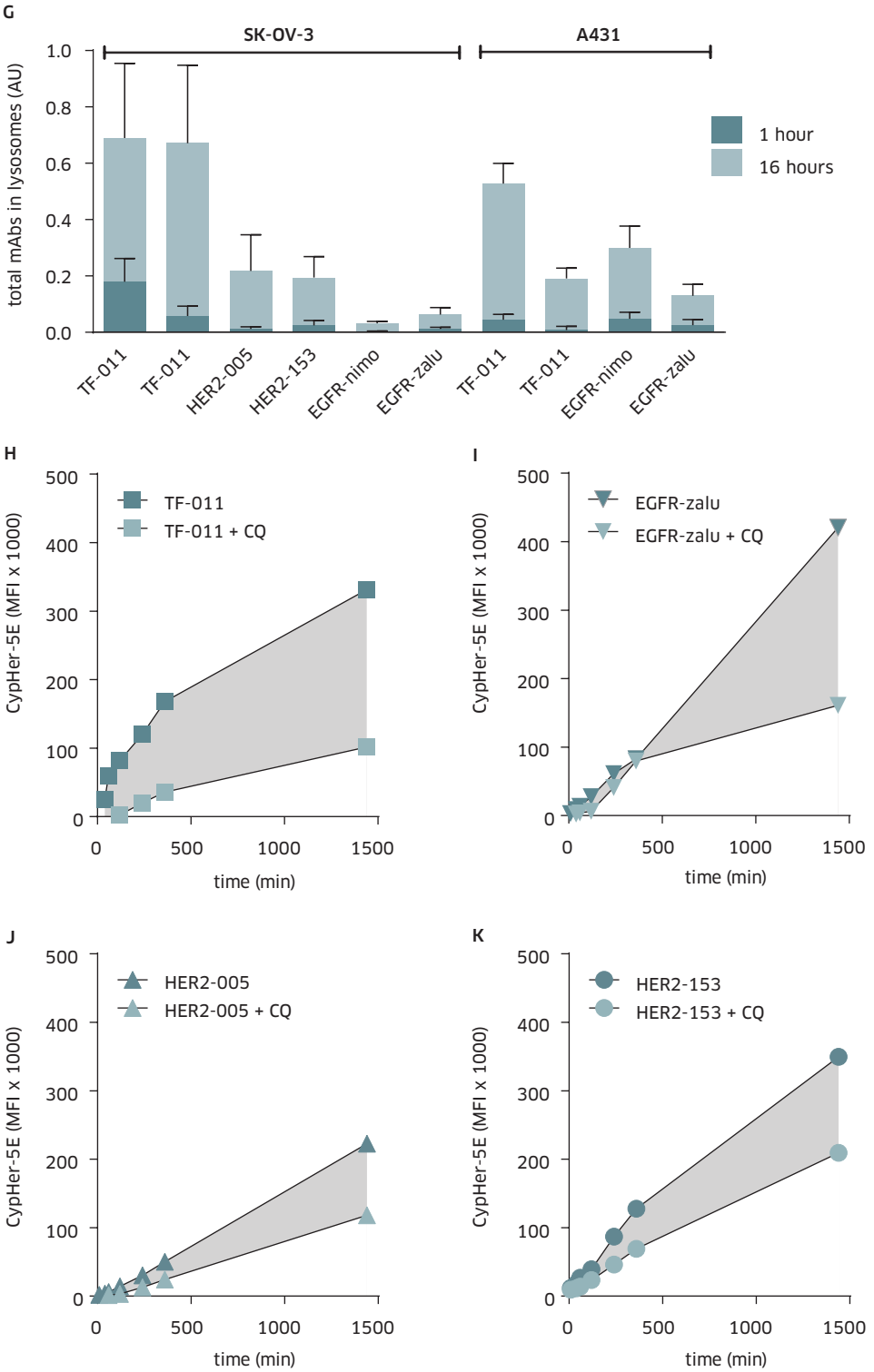
G
SK-OV-3
A431
total mAbs in lysosomes (AU)
1.0
0.8
0.6
0.4
0.2
0.0
1 hour
16 hours
TF-011
TF-011
HER2-005
HER2-153
EGFR-nimo
EGFR-zalu
TF-011
TF-011
EGFR-nimo
EGFR-zalu
H
CypHer-5E (MFI x 1000)
TF-011
TF-011 + CQ
time (min)
I
EGFR-zalu
EGFR-zalu + CQ
J
HER2-005
HER2-005 + CQ
K
HER2-153
HER2-153 + CQ
0
100
200
300
400
500
1000
1500

sosomal colocalisation, but TF mAbs were most abundantly present in lysosomes (Figure 3B, D, F and G). Additionally, receptor distribution was tested after antibody treatment (Supplementary Figure S2). Both TF-antibodies significantly increased the amount of TF in endosomes and lysosomes of SK-OV-3 and A431 cells. EGFR mAbs zalutumumab and nimotuzumab also enhanced endosomal and lysosomal colocalisation of EGFR in A431 cells. In contrast, cellular distribution of HER2 was hardly affected by HER2 antibodies 005 and 153.

The more rapid lysosomal colocalisation of TF-mAbs, led us to investigate TF mediated internalization and lysosomal targeting in more detail. By conjugating TF, HER2 and EGFR mAbs with CypHer5E, a dye that becomes fluorescent at acidic pH, we were able to follow internalization and lysosomal colocalisation over time. Both endosomes and lysosomes are acidic environments that induce fluorescence of CypHer5E. To distinguish between fluorescence resulting from endosomal and lysosomal transport, SK-OV-3 cells were preincubated with chloroquine, which inhibits the acidification and fusion of endosomes with lysosomes [34]. Thus, inhibition of CypHer5E fluorescence by chloroquinine is indicative of lysosomal transport. This was most evident for TF-011 (Figure 3H). Whereas fluorescence of CypHer5E conjugated mAbs 005, 153 and zalutumumab was only inhibited after 24 hours incubation (Figure 3I-K), fluorescence of TF-011-CypHer5E was already inhibited within one hour. This shows that TF bound antibodies were rapidly transported to lysosomes, while lysosomal transport of EGFR and HER2 mAbs was relatively slow.

In vitro cytotoxicity induced by duostatin-3-conjugated TF, EGFR and HER2 antibodies

To investigate whether the more rapid lysosomal targeting observed with TF mAbs, results in increased cytotoxicity of TF-directed ADCs, we conjugated antibodies TF-011, 005 and zalutumumab with duostatin-3 using a valine-citrulline linker that is cleaved by intracellular proteases such as cathepsin B. Duostatin-3 is an antimitotic agent that inhibits cell division by blocking of tubulin polymerization. Unlike vcMMAE, duostatin-3 can not kill neighbouring tumor cells when the drug is released from the antibody. This was also demonstrated in Figures 4B, D and F, where duostatin-3 conjugated antibodies did not induce bystander kill. Whereas TF-011-MMAE induced potent bystander kill which was in line with results published previously [4,33]. To study the target requirements needed for efficient intracellular drug delivery, a drug-linker that only affects antigen expressing cells was preferred. Figure 4A, C and E, show that duostatin-3 conjugated HER2 and EGFR antibodies only induced cytotoxicity when tumor cells highly overexpress their targets HER2 (AU565 and SK-OV-3) and EGFR (A431 and AU565) respectively. Viability of tumor cells that display moderate overexpression of HER2 (A431) or EGFR (SK-OV-3) was hardly affected. In contrast, TF-mAbs conjugated with duostatin-3 induced cytotoxicity in all tested cell lines, including cells that express less than 20,000 TF molecules/cell. Analysis of

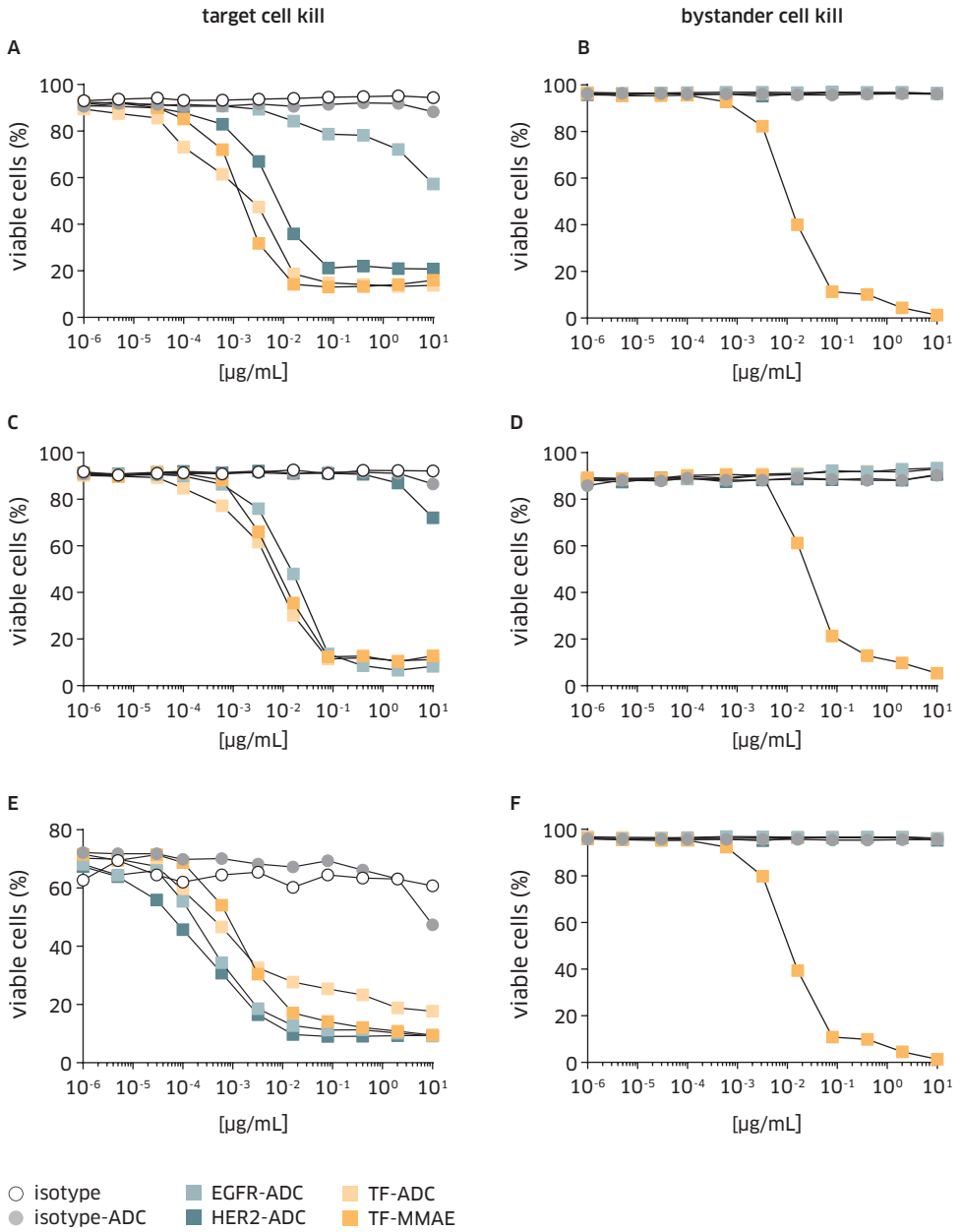

FIGURE 4 *Cytotoxicity of TF-ADC, EGFR-ADC, HER2-ADC and TF-011-MMAE in vitro.* SK-OV-3 **(A-B)**, A431 **(C-D)** and AU565 **(E-F)** cells were seeded in 96-wells tissue culture plates together with CFSE-labeled Jurkat cells. Serially diluted ADCs and isotype control antibody were added to the cells. After 4-days incubation at 37°C viability was assessed on a flow cytometer. Target cell kill was plotted as the percentage of viable CFSE- SK-OV-3, A431, and AU565 cells (left panel). Bystander kill was plotted as the percentage of viable CFSE+ cells (right panel).

TF-expression in SK-OV-3 cells that survived TF-ADC-treatment demonstrated that TF expression was similar before and after treatment (Table 2 and supplementary figure S3). However, the proliferation-rate of the surviving cells was reduced, as indicated by the high CFSE fluorescence of the surviving cells. This indicates that lack of efficacy against these cells was caused by their low proliferation-rate, rather than lack of target expression.

Anti-tumor activity of duostatin-3-conjugated TF, EGFR and HER2 antibodies *in vivo*

Finally, the effect of ADC treatment on tumor growth was assessed *in vivo*. The ADCs were compared in two different tumor xenograft models, starting with the breast cancer model HCC1954 (Figure 5A-B) which highly overexpressed HER2 and TF (Table 1). Figure 5B demonstrates that treatment with a single dose of 1 mg/kg TF-ADC resulted in significant inhibition of HCC1954 tumor growth as compared to animals treated with isotype control ADC. At the same dose, HER2-ADC had no effect on tumor growth. At 4 mg/kg, both ADCs induced tumor regression, which was sustained until at least 67 days post treatment.

Using the epidermal carcinoma model A431, ADCs targeting TF and EGFR were compared (Figure 5C-D). A single dose of 1 mg/kg TF-ADC induced significant inhibition of tumor growth, which was increased at 4 mg/kg. EGFR-ADC only reduced tumor growth at 4 mg/kg, a dose at which TF-ADC treatment was significantly more effective. Overall, TF-ADC treatment induced significant inhibition of tumor growth. Despite the reduced expression of TF as compared to HER2 and EGFR, TF-ADC outperformed HER2- and EGFR- ADCs. Hence these data demonstrate the potential of TF as tumor target for an ADC approach.

DISCUSSION

Antibodies conjugated with tubulin inhibitors have demonstrated impressive preclinical and clinical anti-tumor activity [1,20,35,36]. However, the optimal target characteristics for ADC development are not entirely clear. Most ADCs are dependent on internalization and lysosomal targeting to release their cytotoxic compound. Thus the internalization characteristics of a tumor target may greatly contribute to the efficacy of ADCs directed against that target. In addition, binding of antibodies or ADCs to specific tumor targets may change the internalization characteristics of the tumor target. In this study, the internalization characteristics of three different tumor targets, TF, EGFR and HER2, as well as antibodies and ADCs specific for those targets, were compared. Internalization, lysosomal sorting and intracellular degradation of the three proteins were analysed in absence and presence of monoclonal antibodies. The combination of TF and antibody TF-011 was the only combination demonstrating efficacy in all assays. TF demonstrated significant and constitutive

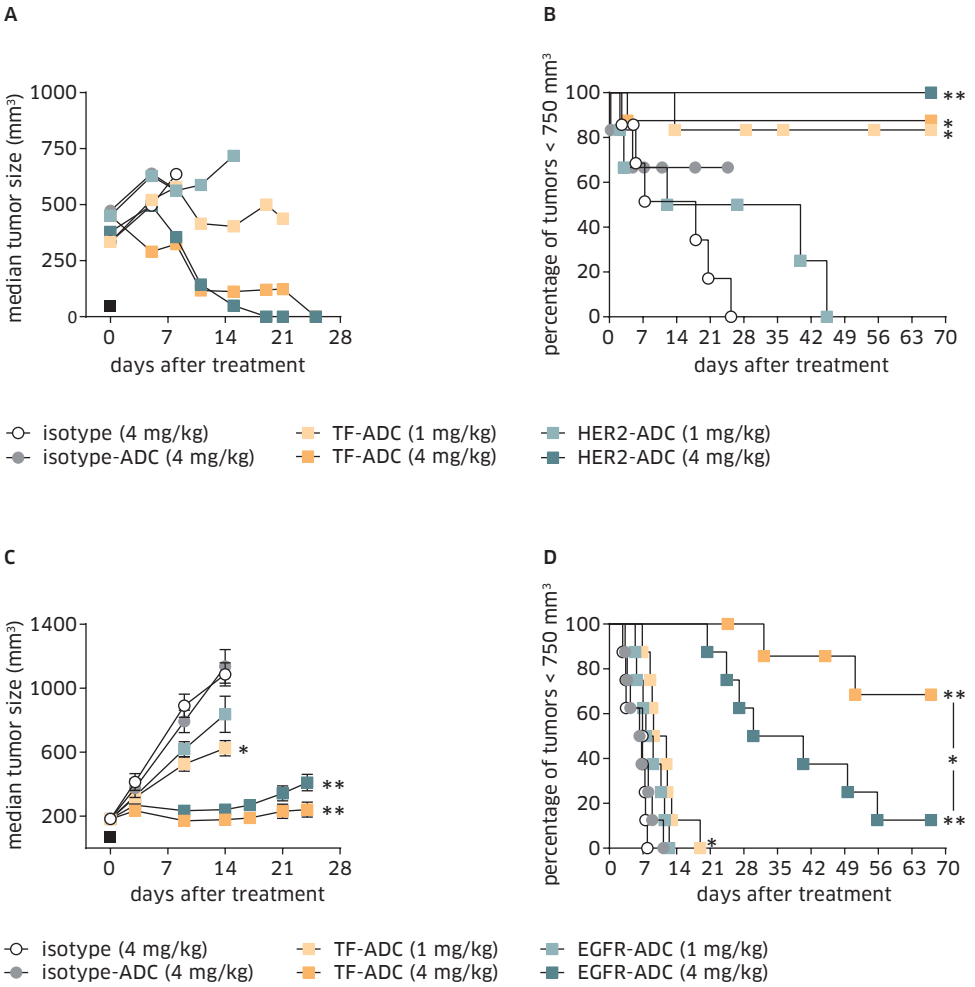

FIGURE 5 *Efficacy of TF-ADC, HER2-ADC and EGFR-ADC in tumor xenograft models.* Mice were inoculated subcutaneously with 5 x 10^6 HCC1954 **(A-B)** or A431 **(C-D)** cells. When average tumor volume reached >200 mm^3, mice were divided in groups of 7 mice with equal tumor size distribution and injected intraperitoneally at indicated time points with 4 mg/kg or 1 mg/kg mAb or ADC. Tumors were measured twice a week by using calipers, and the median **(A)** or mean ± SE **(C)** tumor volume (mm^3) was plotted against time, as well as time to progression indicated by the percentage of tumors <750mm^3 **(B)** or <500mm^3 **(D)**. In the HCC1954 model, some mice developed ulcerations unrelated to tumor size or Ab-treatment. These mice were withdrawn from the study as indicated by the censored data points **(B)**. Median tumor volumes were not calculated when more than 3 mice had been withdrawn **(A)**. *P<0.05, ** P<0.001

internalization, lysosomal colocalisation and degradation in tumor cells, all of which were increased upon incubation with TF-011. Given the potential of TF as target for an ADC approach, TF-, EGFR- and HER2- mAbs were conjugated with the cleavable linker-drug vcDuostatin-3, generating ADCs that provide specific tumor targeting with a payload only affecting proliferating cells. We found that TF-ADC outperformed HER2-ADC and EGFR-ADC in two different tumor xenograft models.

Quantitative flow cytometry analysis of tumor cell lines revealed that, like EGFR and HER2, TF can be aberrantly expressed on tumor cells. Compared with normal melanocytes, more than 1000-fold increased TF expression has been reported on metastatic human melanoma cells [37]. In the tumor models selected here, extracellular expression of TF was lower compared to EGFR and HER2. However, despite the lower antigen expression, the anti-tumor activity of TF-ADC was more potent compared to HER2- and EGFR- ADCs. This can be explained by the efficient transport of TF-011 from the plasma membrane into lysosomes of tumor cells as demonstrated with confocal microscopy. Previous publications also indicate that TF has a higher turnover rate compared to EGFR and HER2. Hamik et al. demonstrated that the half-life of TF on monocytes was 3.7 hours, which could be reduced to 1.3 hours when TF was bound by tissue factor protein inhibitor and FVII [38]. Unstimulated EGFR and HER2 on the other hand have a half-life of 6-24 hours depending on the cell line used [39]. Since TF is the main physiological initiator of the coagulation cascade, which represents a system that needs to be tightly regulated it makes sense that TF is more efficiently internalized and degraded compared to EGFR and HER2.

	Cytotoxicity (number of events)	Antigen expression (MFI APC)	Proliferation rate (MFI CFSE)
EGFR	40100	26613	65493
EGFR + EGFR-ADC	17858	21380	93951
HER2	39836	90735	65493
HER2 + HER2-ADC	7034	76490	122213
TF	42522	51237	65493
TF + TF-ADC	2403	45816	175662

TABLE 2 *Flow cytometry analysis of SK-OV-3 cells after ADC-treatment.* SK-OV-3 cells were labeled with CFSE, a dye that is stably fluorescent and that is transferred to daughter cells upon cell division with its fluorescence being halved. Thus reduced CFSE fluorescence indicates SK-OV-3 proliferation. CFSE labeled cells were treated 3 days with 2 µg/mL ADC after which cytotoxicity was analysed as well as expression of the antigen targeted by the respective ADC. Cytotoxicity was expressed as number of events measured on a flow cytometer. Antigen expression was detected with mouse anti-HER2, anti-EGFR and anti-TF antibodies in combination with APC-conjugated rabbit anti-mouse and depicted as MFI of APC.

Internalization of TF has been studied previously [16,40] and is believed to be an active process which can be enhanced through binding of FVIIa. We did not observe FVIIa mediated internalization of TF. Instead we found that TF was constitutively being turned over on tumor cells, a process which was not influenced by presence of FVIIa. Most studies focussing on internalization of TF:FVIIa complexes made use of radiolabelled FVIIa [16,31,41]. Our studies, using TF expression as read out, demonstrate that FVIIa most likely piggy-backs with internalizing TF. Various cancer cells including ovarian cancer cells have been reported to produce FVII themselves [42], however we did not detect FVII production in culture supernatant (data not shown).

Although the more rapid internalization and lysosomal targeting of TF seem fundamental for effective ADC treatment, the potent anti-tumor effect of TF-ADC can not be fully ascribed to the target characteristics of TF alone. Antibody selection plays an important role as well. This was illustrated by the increased internalization and lysosomal targeting observed with TF-011. While TF-011 is expected to crosslink extracellular TF, Fab-011 and FVII lack the ability to crosslink TF, indicating that mAb-induced crosslinking may be critical to increase downmodulation of extracellular TF. TF-111 on the other hand only seems to crosslink TF when highly overexpressed. Moreover differential antibody binding at low pH may influence intracellular trafficking of ADCs and consequently increase their lysosomal transport. Flow cytometry analysis of antibody binding at pH6 and pH7.4 revealed no differences in binding at reduced pH (Supplementary Table S1). Also no substantial differences were observed between apparent affinities of antibodies targeting TF, EGFR and HER2 (Supplementary Table S1). The low affinity EGFR mAb nimotuzumab was an exception to this and showed low apparent affinity binding to EGFR expressing cells (EC50 value 15.6 nM). Furthermore, inhibition of receptor signalling and engagement of immune effector cells may contribute to the anti-tumor activity of ADCs as well. However, treatment of established A431 xenografts with comparable dosing of unconjugated mAbs induced significantly less (EGFR-mAb [43]) or no (TF-mAbs [4]), inhibition of tumor growth. The unconjugated HER2 antibody 005 demonstrated modest inhibition of *in vivo* tumor growth, when tested at >10-fold higher dose in a high HER2 expressing tumor model (data not shown).

While EGFR and HER2 belong to a family of receptor tyrosine kinases, for which endocytic trafficking has been extensively investigated, TF is a member of the class II cytokine receptor superfamily. To date, little is known about intracellular trafficking of these proteins and their potential use in ADC based therapy. Our data indicate that such targets can be very attractive for an ADC-approach because of their rapid internalization, lysosomal targeting and degradation, which may be inherent to their physiological roles in regulating immune responses [44,45]. Taken together, these

data support the use of TF-ADC in cancer therapy and a clinical study is underway to assess the safety and efficacy of TF-011-MMAE, an auristatin-conjugate of antibody TF-011, for the treatment of patients with solid cancers.

Acknowledgements

We would like to thank Maarten Dokter, Hendrik ten Napel and Ester van 't Veld for technical support and Esther Breij for reviewing the manuscript.

REFERENCE LIST

1 Senter PD, Sievers EL: The discovery and development of brentuximab vedotin for use in relapsed Hodgkin lymphoma and systemic anaplastic large cell lymphoma. *Nat Biotechnol* 2012, 30(7):631-637.

2 LoRusso PM, Weiss D, Guardino E, Girish S, Sliwkowski MX: Trastuzumab emtansine: a unique antibody-drug conjugate in development for human epidermal growth factor receptor 2-positive cancer. *Clin Cancer Res* 2011, 17(20):6437-6447.

3 Burris HA: Trastuzumab emtansine: a novel antibody-drug conjugate for HER2-positive breast cancer. *Expert Opin Biol Ther* 2011, 11(6):807-819.

4 Breij EC, de Goeij BE, Verploegen S, Schuurhuis DH, Amirkhosravi A, Francis J, Miller VB, Houtkamp M, Bleeker WK, Satijn D *et al*: An antibody-drug conjugate that targets tissue factor exhibits potent therapeutic activity against a broad range of solid tumors. *Cancer Res* 2014, 74(4):1214-1226.

5 Goldin-Lang P, Tran QV, Fichtner I, Eisenreich A, Antoniak S, Schulze K, Coupland SE, Poller W, Schultheiss HP, Rauch U: Tissue factor expression pattern in human non-small cell lung cancer tissues indicate increased blood thrombogenicity and tumor metastasis. *Oncol Rep* 2008, 20(1):123-128.

6 Shigemori C, Wada H, Matsumoto K, Shiku H, Nakamura S, Suzuki H: Tissue factor expression and metastatic potential of colorectal cancer. *Thromb Haemost* 1998, 80(6):894-898.

7 Gonzalez-Gronow M, Gawdi G, Pizzo SV: Tissue factor is the receptor for plasminogen type 1 on 1-LN human prostate cancer cells. *Blood* 2002, 99(12):4562-4567.

8 Patry G, Hovington H, Larue H, Harel F, Fradet Y, Lacombe L: Tissue factor expression correlates with disease-specific survival in patients with node-negative muscle-invasive bladder cancer. *Int J Cancer* 2008, 122(7):1592-1597.

9 Uno K, Homma S, Satoh T, Nakanishi K, Abe D, Matsumoto K, Oki A, Tsunoda H, Yamaguchi I, Nagasawa T *et al*: Tissue factor expression as a possible determinant of thromboembolism in ovarian cancer. *Br J Cancer* 2007, 96(2):290-295.

10 Cocco E, Hu Z, Richter CE, Bellone S, Casagrande F, Bellone M, Todeschini P, Krikun G, Silasi DA, Azodi M *et al*: hI-con1, a factor VII-IgGFc chimeric protein targeting tissue factor for immunotherapy of uterine serous papillary carcinoma. *Br J Cancer* 2010, 103(6):812-819.

11 Cocco E, Varughese J, Buza N, Bellone S, Glasgow M, Bellone M, Todeschini P, Carrara L, Silasi DA, Azodi M *et al*: Expression of Tissue factor in Adenocarcinoma and Squamous Cell Carcinoma of the Uterine Cervix: Implications for immunotherapy with hI-con1, a factor VII-IgGFc chimeric protein targeting tissue factor. *BMC Cancer* 2011, 11(263).

12 Khorana AA, Ahrendt SA, Ryan CK, Francis CW, Hruban RH, Hu YC, Hostetter G, Harvey J, Taubman MB: Tissue factor expression, angiogenesis, and thrombosis in pancreatic cancer. *Clin Cancer Res* 2007, 13(10):2870-2875.

13 Wojtukiewicz MZ, Zacharski LR, Rucinska M, Zimnoch L, Jaromin J, Rozanska-Kudelska M, Kisiel W, Kudryk BJ: Expression of tissue factor and tissue factor pathway inhibitor in situ in laryngeal carcinoma. *Thromb Haemost* 1999, 82(6):1659-1662.

14 Hamada K, Kuratsu J, Saitoh Y, Takeshima H, Nishi T, Ushio Y: Expression of tissue factor in glioma. *Noshuyo Byori* 1996, 13(2):115-118.

15 Jiang X, Zhu S, Panetti TS, Bromberg ME: Formation of tissue factor-factor VIIa-factor Xa complex induces activation of the mTOR pathway which regulates migration of human breast cancer cells. *Thromb Haemost* 2008, 100(1):127-133.

16 Hansen CB, Pyke C, Petersen LC, Rao LV: Tissue factor-mediated endocytosis, recycling, and degradation of factor VIIa by a clathrin-independent mechanism not requiring the cytoplasmic domain of tissue factor. *Blood* 2001, 97(6):1712-1720.

17 Mandal SK, Pendurthi UR, Rao LV: Cellular localization and trafficking of tissue factor. *Blood* 2006, 107(12):4746-4753.

18 Schecter AD, Giesen PL, Taby O, Rosenfield CL, Rossikhina M, Fyfe BS, Kohtz DS, Fallon JT, Nemerson Y, Taubman MB: Tissue factor expression in human arterial smooth muscle cells. TF is present in three cellular pools after growth factor stimulation. *J Clin Invest* 1997, 100(9):2276-2285.

19 Kasthuri RS, Taubman MB, Mackman N: Role of tissue factor in cancer. *J Clin Oncol* 2009, 27(29):4834-4838.

20 Verma S, Miles D, Gianni L, Krop IE, Welslau M, Baselga J, Pegram M, Oh D-Y, Diéras V, Guardino E *et al*: Trastuzumab Emtansine for HER2-Positive Advanced Breast Cancer. *N Eng J Med* 2012, 367(19):1783-1791.

21 Fishwild DM, O'Donnell SL, Bengoechea T, Hudson DV, Harding F, Bernhard SL, Jones D, Kay RM, Higgins KM, Schramm SR *et al*: High-avidity human IgG kappa monoclonal antibodies from a novel strain of minilocus transgenic mice. *Nat Biotechnol* 1996, 14(7):845-851.

22 de Goeij BE, Peipp M, De Haij S, van den Brink EN, Kellner C, Riedl T, de Jong R, Vink T, Strumane K, Bleeker WK *et al*: HER2 monoclonal antibodies that do not interfere with receptor heterodimerization-mediated signaling induce effective internalization and represent valuable components for rational antibody-drug conjugate design. *MAbs in press [published online January 3, 2014; doi:104161/mabs27705]*.

23 Bleeker WK, Lammerts van Bueren JJ, van Ojik HH, Gerritsen AF, Pluyter M, Houtkamp M, Halk E, Goldstein J, Schuurman J, van Dijk MA *et al*: Dual mode of action of a human anti-epidermal growth factor receptor monoclonal antibody for cancer therapy. *J Immunol* 2004, 173(7):4699-4707.

24 Ramakrishnan MS, Eswaraiah A, Crombet T, Piedra P, Saurez G, Iyer H, Arvind AS: Nimotuzumab, a promising therapeutic monoclonal for treatment of tumors of epithelial origin. *MAbs* 2009, 1(1):41-48.

25 Levkowitz G, Waterman H, Zamir E, Kam Z, Oved S, Langdon WY, Beguinot L, Geiger B, Yarden Y: c-Cbl/Sli-1 regulates endocytic sorting and ubiquitination of the epidermal growth factor receptor. *Genes Dev* 1998, 12(23):3663-3674.

26 Poncelet P, Carayon P: Cytofluorometric quantification of cell-surface antigens by indirect immunofluorescence using monoclonal antibodies. *J Immunol Methods* 1985, 85(1):65-74.

27 Labrijn AF, Meesters JI, de Goeij BE, van den Bremer ET, Neijssen J, van Kampen MD, Strumane K, Verploegen S, Kundu A, Gramer MJ *et al*: Efficient generation of stable bispecific IgG1 by controlled Fab-arm exchange. *Proc Natl Acad Sci U S A* 2013, 110(13):5145-5150.

28 Mandal SK, Pendurthi UR, Rao LV: Tissue factor trafficking in fibroblasts: involvement of protease-activated receptor-mediated cell signaling. *Blood* 2007, 110(1):161-170.

29 Vincent MJ, Bergeron E, Benjannet S, Erickson BR, Rollin PE, Ksiazek TG, Seidah NG, Nichol ST: Chloroquine is a potent inhibitor of SARS coronavirus infection and spread. *Virol J* 2005, 2::69.

30 Mellman I: Endocytosis and molecular sorting. *Annu Rev Cell Dev Biol* 1996, 12:575-625.

31 Iakhiaev A, Pendurthi UR, Voigt J, Ezban M, Vijaya Mohan Rao L: Catabolism of factor VIIa bound to tissue factor in fibroblasts in the presence and absence of tissue factor pathway inhibitor. *J Biol Chem* 1999, 274(52):36995-37003.

32 Lammerts van Bueren JJ, Bleeker WK, Bogh HO, Houtkamp M, Schuurman J, van de Winkel JG, Parren PW: Effect of target dynamics on pharmacokinetics of a novel therapeutic antibody against the epidermal growth factor receptor: implications for the mechanisms of action. *Cancer Res* 2006, 66(15):7630-7638.

33 Smith LM, Nesterova A, Alley SC, Torgov MY, Carter PJ: Potent cytotoxicity of an auristatin-containing antibody-drug conjugate targeting melanoma cells expressing melanotransferrin/p97. *Mol Cancer Ther* 2006, 5(6):1474-1482.

34 Koh YH, von Arnim CA, Hyman BT, Tanzi RE, Tesco G: BACE is degraded via the lysosomal pathway. *J Biol Chem* 2005, 280(37):32499-32504.

35 Flygare JA, Pillow TH, Aristoff P: Antibody-drug conjugates for the treatment of cancer. *Chem Biol Drug Des* 2013, 81(1):113-121.

36 Alley SC, Okeley NM, Senter PD: Antibody-drug conjugates: targeted drug delivery for cancer. *Curr Opin Chem Biol* 2010, 14(4):529-537.

37 Mueller BM, Reisfeld RA, Edgington TS, Ruf W: Expression of tissue factor by melanoma cells promotes efficient hematogenous metastasis. *Proc Natl Acad Sci U S A* 1992, 89(24):11832-11836.

38 Hamik A, Setiadi H, Bu G, McEver RP, Morrissey JH: Down-regulation of monocyte tissue factor mediated by tissue factor pathway inhibitor and the low density lipoprotein receptor-related protein. *J Biol Chem* 1999, 274(8):4962-4969.

39 Sorkin A, Goh LK: Endocytosis and intracellular trafficking of ErbBs. *Exp Cell Res* 2008, 314(17):3093-3106.

40 Rao LVM, Pendurthi UR: Regulation of tissue factor-factor VIIa expression on cell surfaces: A role for tissue factor-factor VIIa endocytosis. *Mol Cell Biochem* 2003, 253(1-2):131-140.

41 Chang GT, Kisiel W: Internalization and degradation of recombinant human coagulation factor VIIa by the human hepatoma cell line HuH7. *Thromb Haemost* 1995, 73(2):231-238.

42 Yokota N, Koizume S, Miyagi E, Hirahara F, Nakamura Y, Kikuchi K, Ruf W, Sakuma Y, Tsuchiya E, Miyagi Y: Self-production of tissue factor-coagulation factor VII complex by ovarian cancer cells. *Br J Cancer* 2009, 101(12):2023-2029.

43 Overdijk MB, Verploegen S, van den Brakel JH, Lammerts van Bueren JJ, Vink T, van de Winkel JG, Parren PW, Bleeker WK: Epidermal growth factor receptor (EGFR) antibody-induced antibody-dependent cellular cytotoxicity plays a prominent role in inhibiting tumorigenesis, even of tumor cells insensitive to EGFR signaling inhibition. *J Immunol* 2011, 187(6):3383-3390.

44 Ragimbeau J, Dondi E, Alcover A, Eid P, Uze G, Pellegrini S: The tyrosine kinase Tyk2 controls IFNAR1 cell surface expression. *EMBO J* 2003, 22(3):537-547.

45 Wei SH, Ming-Lum A, Liu Y, Wallach D, Ong CJ, Chung SW, Moore KW, Mui AL: Proteasome-mediated proteolysis of the interleukin-10 receptor is important for signal downregulation. *J Interferon Cytokine Res* 2006, 26(5):281-290.

SUPPLEMENTARY METHODS

Quantitative determination of cell surface antigens.

Qifikit (DAKO) was used to detect and quantify cell surface expression of TF, HER2 and EGFR, according to manufacturer's protocol (1). In brief; cells were stained with 10 µg/mL mouse anti-human TF (CLB), mouse anti-human HER2 (R&D), mouse anti-human EGFR (BD), following incubation with polyclonal goat anti-mouse IgG FITC (DAKO). In parallel a series of bead populations, containing a well-defined number of antibody molecules per bead, was stained with the polyclonal goat anti-mouse IgG FITC antibody. Mean fluorescence intensities (MFI) were measured using flow cytometry, and a calibration curve with the MFI of the individual bead populations was plotted against the number of mAb molecules on the beads. This curve was used to interpolate the number of TF, HER2 and EGFR molecules per cell.

Duostatin-3 synthesis

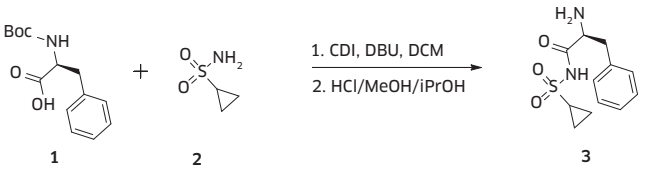

PREPARATION OF COMPOUND 3 To a solution of Boc-L-phenylalanine **1** (5.36 g, 20.2 mmol) in 30 mL of methylene chloride (DCM), carbonyldiimidazole (CDI, 4.26 g, 26.3 mmol) was added and stirred for 1 hour. Then added a solution of **2** (3.67 g, 30.3 mmol) and 2,4-diaminobutyric acid (DBU, 4.5 mL, 30 mmol) in 15 mL of DCM. The mixture was heated at 40°C for 16 hours. The mixture was diluted with 60 mL of DCM and 40 mL of water, then neutralized to pH 7 with conc. HCl. The DCM extract was collected, washed with 0.2M HCl (60 mL), then with brine (60 mL), dried over Na^2SO^4, and evaporated to give 7.47 g of Boc-protected sulfonamide. This material was suspended in 40 mL of methanol, then 200 mL of 6N HCl/isopropanol was added and the mixture was stirred for 2 hours. The solvent was evaporated under vacuum, 100 mL of ether was then added. The precipitate was collected by filtration and dried to give compound **3** as HCl salt (5.93 g, 96%); MS m/z 269.1 (M+H).

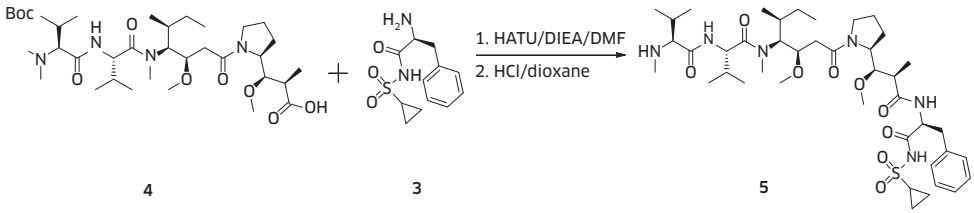

PREPARATION OF COMPOUND 5 To a solution of compound **4** (1.09 g, 1.6 mmol) in 10 mL of N,N-Dimethylformamide (DMF) was added 2-(lH-7-azabenzotriazol-l-yl)-l,l ,3,3-tetramethyl uranium hexafluorophosphate (HATU, 0.61 g, 1.6 mmol), diisopropylethylamine (DIEA, 0.56 mL), and compound **3** (0.49 g, 1.6 mmol) in that order. The mixture was stirred for 1 hour and diluted with 100 mL of water and 4 mL of acetic acid. The precipitate was collected by filtration, dried under vacuum and added to 10 mL of 4M HCl/dioxane. After 30 min, 200 mL of ether was added and insoluble precipitate was collected and purified by HPLC to give compound **5** as tetrahydrofuran salt (TFA, 1.3 g, 88%); MS m/z 835.5 (M+H). Compound **5** is referred to as duostatin-3 throughout the manuscript.

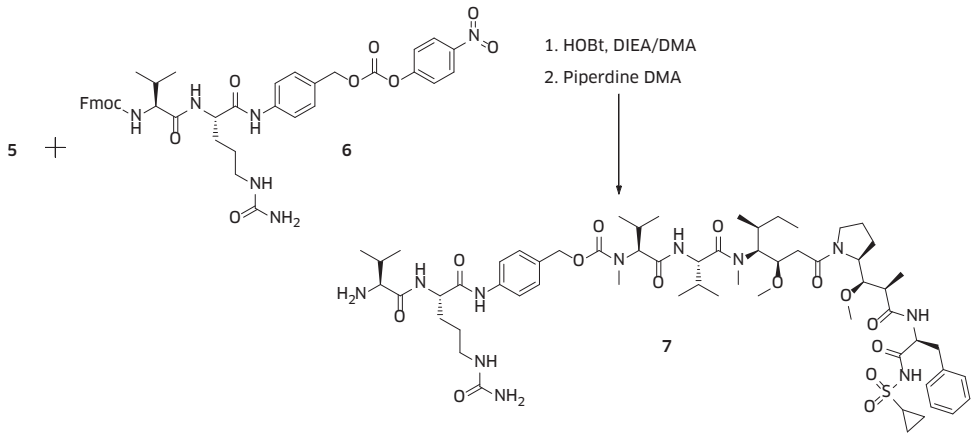

PREPARATION OF COMPOUND 7 To a solution of compound **5** (500 mg, 0.527 mmol) in 5 mL of DMF was added compound **6** (483 mg, 0.631 mmol), N-Hydroxybenzotriazole (HOBt, 40 mg, 0.296 mmol), and DIEA (0.27 mL). The mixture was stirred for 16 hours after which 0.4 mL of piperidine was added. After 1 hour, the mixture was diluted with 100 mL of ether and the precipitate was collected and dried to give compound **7** as HCl salt (640 mg, 95 %); MS m/z 1240.7 (M+H).

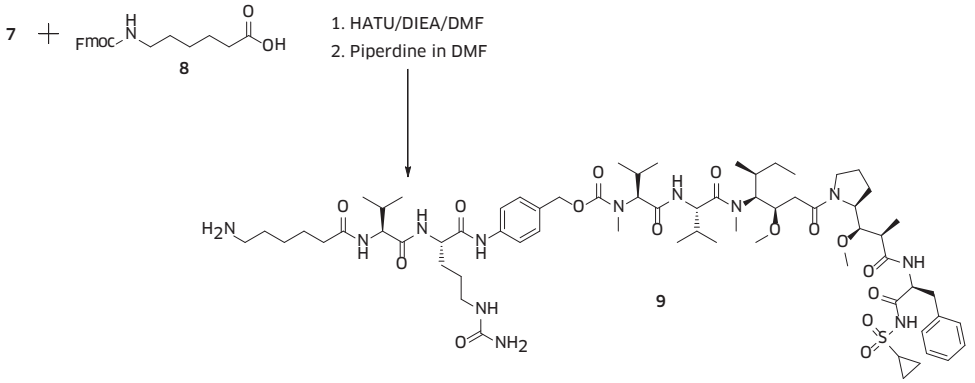

PREPARATION OF COMPOUND 9 To a solution of compound **8** (219 mg, 0.62 mmol) in 5 mL of DMF was added HATU (236 mg, 0.62 mmol), DIEA (0.15 mL), and compound **7** (316 mg, 1.6 mmol), respectively. After 1 hour, 0.2 mL of piperidine was added and the mixture was stirred for 30 min, then purified by HPLC to give compound **9** as TFA salt (235 mg, 64 %); MS m/z 1353.8 (M+H).

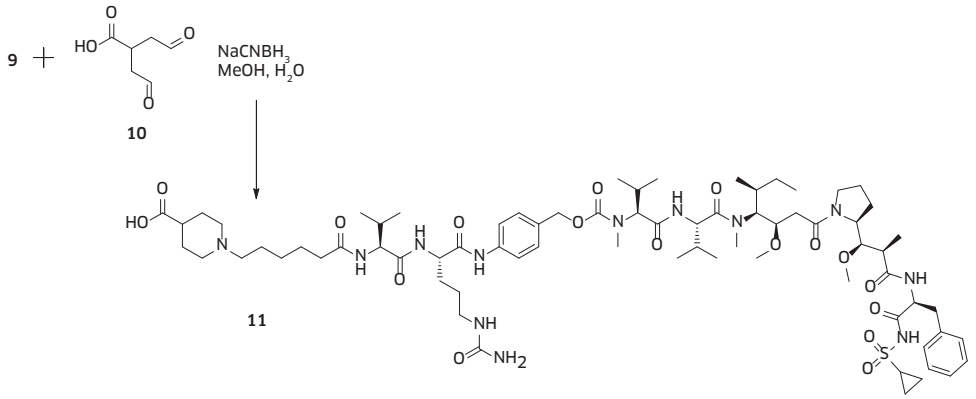

PREPARATION OF COMPOUND 11 To a solution of compound **9** (235 mg, 0.16 mmol) in 2 mL of methanol and 1 mL of water was added a solution of dialdehyde **10** (1.6 mL of 0.3M in iPrOH) and NaCNBH3 (180 mg, 2.85 mmol). The mixture was stirred for 2 hours at RT, and then purified by HPLC giving rise to compound **11** as TFA salt (126 mg, 50 %); MS m/z 1465.8 (M+H).

SUPPLEMENTARY TABLE

Antibody	Antigen	EC_{50} pH7.4 (nM)	EC_{50} pH6.0 (nM)
011	TF	0.69	0.61
111	TF	0.49	0.47
005	HER2	1.63	1.10
153	HER2	0.57	0.55
Zalutumumab	EGFR	0.93	1.45
Nimotuzumab	EGFR	15.6	13.8

SUPPLEMENTARY TABLE S1 *Apparent antibody affinities.* Apparent antibody affinities at pH7.4 and 6.0 measured using flow cytometry. SK-OV-3 cells, overexpressing TF, EGFR and HER2 were incubated with TF, EGFR and HER2 antibodies diluted in FACS-buffer at pH7.4 and FACS-buffer adjusted to pH6.0 with NaCl. Antibody binding was detected using a phycoerythrin (PE)-conjugated goat anti-human IgG antibody diluted in FACS-buffer at pH7.4. PE fluorescence was measured on a flow cytometer and EC_{50} values were calculated using GraphPad Prism 5 software.

SUPPLEMENTARY FIGURES

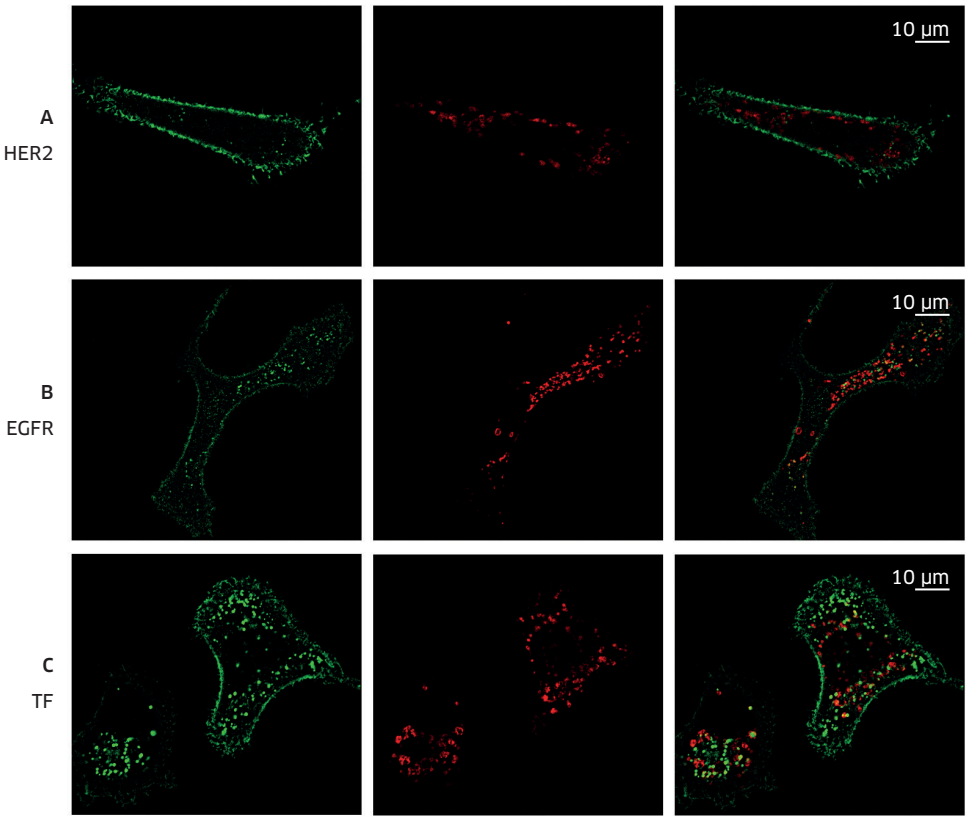

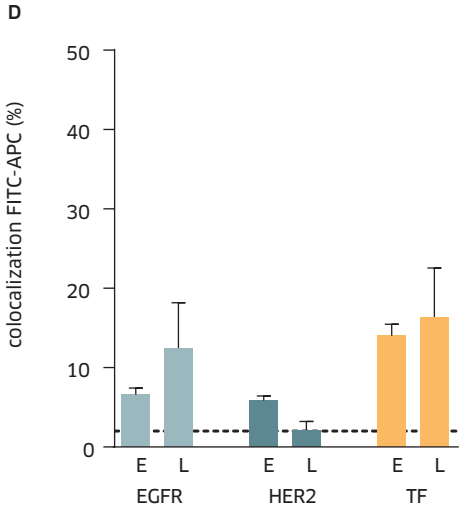

SUPPLEMENTARY FIGURE S1 *Distribution of HER2, EGFR and TF in unstimulated HCC1954 cells.* **(A-C, page 64)** Confocal microscopy images (12-bit) of unstimulated HCC1954 cells. The left panel shows staining of HER2 **(A)**, EGFR **(B)** and TF **(C)** with murine antibodies and goat anti-mouse IgG-FITC (green). In the middle panel lysosomes were stained with mouse anti-human LAMP1-APC (red). The right panel shows the overlay (yellow). **(D)** Quantification of endosomal and lysosomal receptor colocalisation. Each bar represents 4 different 12-bit images ± standard deviation. E=endosomes L=lysosomes.

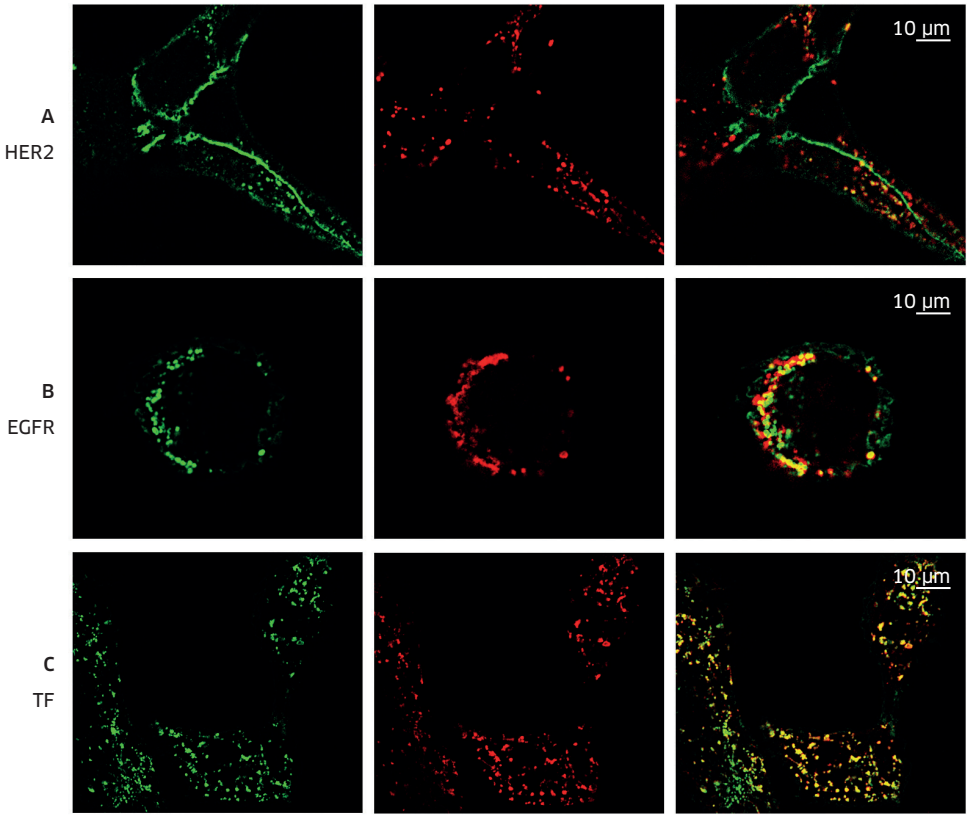
A
HER2
10 µm
B
EGFR
10 µm
C
TF
10 µm

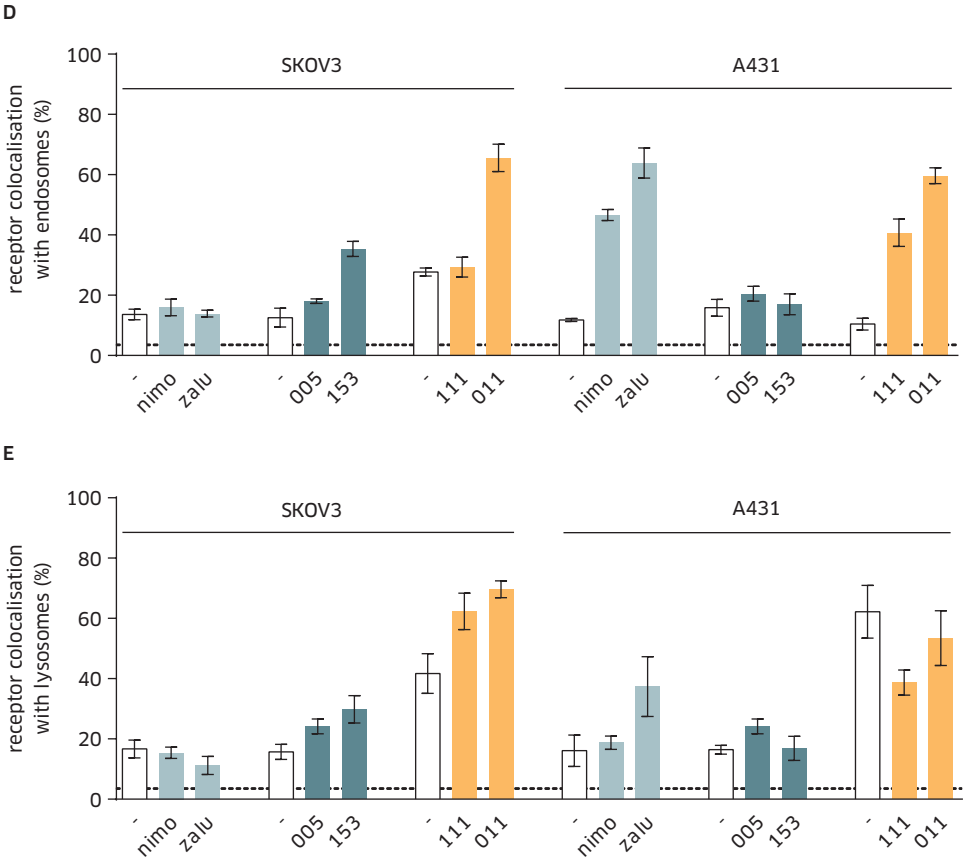

SUPPLEMENTARY FIGURE S2 *Endosomal and lysosomal colocalisation of TF, EGFR and HER2 in tumor cells after treatment with target-specific antibodies.* (**A-C, page 66**) Confocal analysis of SK-OV-3 cells demonstrating enhanced TF colocalisation with the lysosomal marker LAMP1 after incubation with TF-antibodies. Lysosomes were stained with mouse anti-human LAMP1-APC (red, middle panel). EGFR, HER2 and TF were stained with mouse monoclonal antibodies and visualized using goat anti-mouse IgG-FITC (green, left panel). Colocalisation of EGFR, HER2 and TF staining with the lysosomal marker LAMP1 is depicted in the overlay (yellow, right panel). (**D-E**) Pixel intensity of TF, HER2 and EGFR overlapping with **(D)** the endosomalmarker transferrin and **(E)** the lysosomal marker LAMP1, plotted as a percentage of total TF, HER2 and EGFR intensities. Data shown are mean ± standard deviation of 4 images. The dotted line indicates aspecific colocalisation.

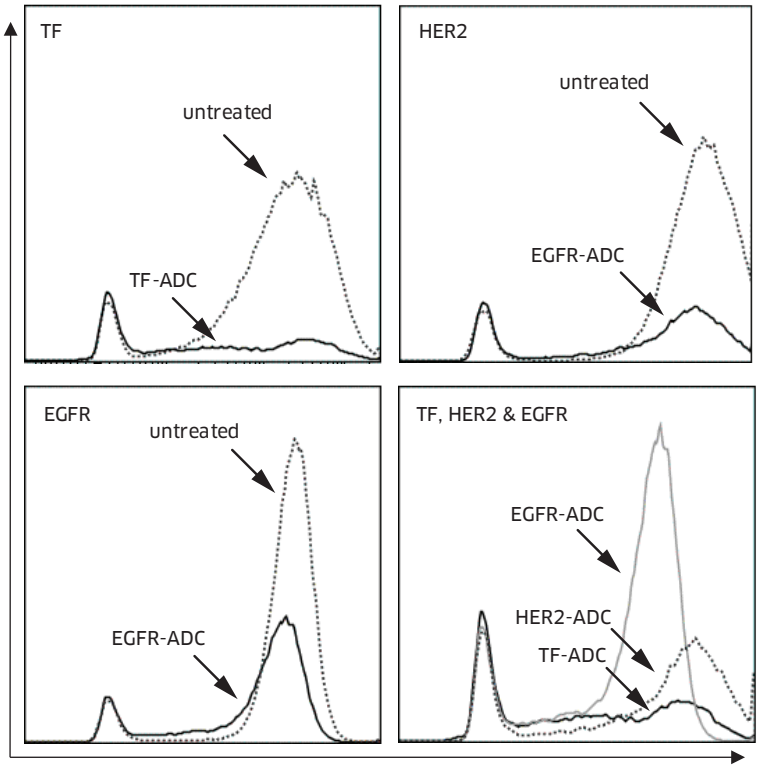

SUPPLEMENTARY FIGURE S3 *Flow cytometry analysis of SK-OV-3 cells after ADC-treatment.* Expression of TF, HER2 and EGFR on SK-OV-3 cells that survived ADC-treatment was analyzed using flow cytometry. Target expression was depicted on the X-axis as fluorescence intensity of APC. The number of surviving cells was depicted on the Y-axis as counts. The APC negative counts represent Jurkat cells that were spiked into each sample. Jurkat cells did not express EGFR, HER2 or TF and were used for quantification purposes.